

Tumor fitness, immune exhaustion and clinical outcomes: impact of immune checkpoint inhibitors

Adrian Bubie(1), Edgar Gonzalez-Kozlova(1), Nicholas Akers(2), Augusto Villanueva (3), Bojan Losic* (4)

1: Department of Genetics and Genomic Sciences, Icahn Institute for Data Science and Genomic Technology, Icahn School of Medicine at Mount Sinai, New York, NY 10029

2: Adaptive biotechnologies, 1551 Eastlake Avenue E, Suite 200, Seattle WA 98102

3: Division of Liver Diseases, Department of Medicine, Liver Cancer Program, Tisch Cancer Institute, Icahn School of Medicine at Mount Sinai, New York, USA.

4: Department of Genetics and Genomic Sciences, Tisch Cancer Institute, Cancer Immunology, Diabetes, Obesity and Metabolism Institute, Icahn Institute for Data Science and Genomic Technology, Icahn School of Medicine at Mount Sinai, New York, NY 10029

*Correspondence to: bojan.losic@mssm.edu

Abstract

Recently proposed tumor fitness measures, based on profiling neoepitopes for reactive viral epitope similarity, have led to improved prediction models of response to immune checkpoint inhibitors in melanoma and small-cell lung cancer. Here we test if this checkpoint based fitness is associated with tumor T-cell infiltration, cytolytic activity (CYT), and abundance (TIL burden) in the treatment naive samples from the same tumor types using data from TCGA. We find no significant correlation between TIL burden or CYT and the proposed neoepitope based fitness measures. Similarly, no significant survival predictive power beyond that of overall patient tumor mutation burden in either cohort is observed. Further, we find suggestive evidence that tumor neoepitopes dominate viral epitopes in putative immunogenicity and drives immune response in liver cancer with hepatitis B virus infection (HBV) in the TCGA.

Significance: In treatment naive patients, our results suggest TIL recruitment and cytolytic activity are essentially driven by tumor neoepitopes, regardless of the presence of viral epitopes. We also find that tumor fitness does not predict patient survival better than tumor mutation burden, unlike a simple measure of CYT.

Introduction

Quantifying tumor fitness modulation by immune selection pressure has assumed a new urgency given the growing need to predict immunotherapy efficacy (1, 2). Immune-based anti-tumoral response is driven in part by T-cell receptor (TCR) recognition of tumor neoantigens, which mainly represent mutated protein epitopes (i.e., neoepitopes) derived from somatic mutations. These neoantigens are presented by host-cell major histocompatibility complex (MHC) molecules to facilitate ‘self’ recognition by TCRs, (**Fig. 1b**). Cancer clones that escape immune recognition can hijack CTLA-4 and PD-1 checkpoint blockade, resulting in heterogeneous tumors with a complex immunogenomic profile which may include immune exhaustion, giving rise to mixed or unfavorable response to immune checkpoint inhibition (1).

Recently, a tumor fitness model has been proposed in the context of the two key components defining the TCR-neoantigen interaction: putative neoantigen immunogenicity and TCR recognition (3). Putative immunogenicity is modeled via a nonlinear function of *in silico* derived MHC-I binding affinities arising from the clonal somatic mutation spectrum, while the TCR recognition likelihood is set to scale with sequence similarity to known, infectious, virally derived epitopes from the Immune Epitope Database (IEDB) (4). Given these assumptions, a combined measure of tumor fitness is then defined as the inverse of the maximum clonal immunogenicity potential \bar{I} weighted by all subclones in the tumor (see Methods, **Fig. 1a**).

Although this model successfully predicts response to checkpoint inhibition in melanoma and small cell lung cancer, it is of interest to investigate its applicability, positive predictive power, and assumptions in the arena of the analogous treatment naive (endogenous) TCGA SKCM and NCLC cohorts. Even though important prognostic biomarkers are not necessarily predictive, substantial evidence has already accumulated about the positive survival effects of cytolytic immune activity in melanoma and lung cancer (10,22), strongly suggesting immune selection pressure significantly modulates treatment naive tumor fitness. Furthermore, parallels drawn between tumor and pathogen evolution may extend beyond the checkpoint setting if they are sufficiently general, and quantifying any limitations of current models may lead to new clues about augmenting neoantigen based models for prognostic or predictive biomarker discovery. Indeed, an attractive testing arena for the assumption of pathogen similarity driving TCR recognition is in samples from patients with HBV-related hepatocellular carcinoma (HCC) within the LIHC cohort in the TCGA. Here, viral antigens and tumor neoantigens are simultaneously present and can be explicitly compared using *in-silico* estimates of binding affinity to patient MHC-I alleles.

In this brief report we show that there is no significant correlation between tumor fitness and immune response signatures, nor is patient survival predicted using tumor fitness better than with ordinary tumor mutation burden (TMB), in either SKCM or NSCLC cohorts. Indeed we show that a simple expression signature capturing tumor-infiltrating T-cell activity (CYT) significantly outperforms TMB in predicting survival in SKCM, and nearly so in NSCLC. Finally, we show that tumor neoantigens actually dominate viral antigens in average putative immunogenicity and furthermore correlate with immune response in the HBV+ HCC LIHC cohort.

Results

Tumor fitness does not correlate with CYT and TIL burden in NSCLC and SKCM

We selected 305 patients with non-small cell lung cancer (NSCLC) and 337 with skin cutaneous and melanoma (SKCM) in the TCGA with matched whole exome sequencing (WES) and RNA-seq data (**Fig. 1a**). Putative tumor neoepitopes ($ic_{50} < 500nM$) with significant homology with viral sequences ($e\text{-value} < 10$) from the IEDB (see

Methods) were found in 204/337 (60%) of SKCM and 221/306 (72%) of NSCLC patients. We found that SKCM patients with viral-like epitopes had a significantly worse survival rate, and correlated with lower TMB (but not CYT), while no survival associations were observed for NSCLC (**Supp. Fig. 3**). However, we also found that maximal clonal immunogenicity \bar{I} (see Methods) does not correlate with TIL burden or CYT in either cohort (**Fig 2a,b**). On the other hand we found significant associations between CYT and TIL burden, for both the NSCLC and SKCM cohorts (**Fig. 2a,b**).

Tumor immunogenicity, cytolytic immune activity, and patient survival

In order to assess if tumor fitness predicted survival in these cohorts, we computed median tumor fitness scores in each patient and found that they did not separate overall survival in either SKCM or NSCLC cohorts (**Fig. 3a,b**). However, we found that the gene signature of immune cytolytic activity (CYT) was significantly associated with survival in these patients. As observed in other studies (5), it is challenging for neoepitope based techniques to predict patient survival better than TMB alone, particularly when regressing out powerful covariates such as clinical tumor stage. To establish the relative predictive power of tumor fitness, we constructed a series of multivariate Cox proportional hazard models for each cohort which included TMB, tumor stage, tumor fitness (\bar{I}), and CYT. For each model, we computed the time dependent Brier score (see Methods; briefly, the weighted average of the squared distances between the observed survival status and the predicted survival probability of a model) and compared the resulting prediction error curves. As shown in Figure 4, tumor fitness does not significantly reduce the prediction error in NSCLC nor SKCM compared to models with TMB alone, while CYT does so in SKCM but not in NSCLC (**Fig. 3c,d**). Computing the integrated Brier scores under cross-validation confirms these results are robust (see supplementary materials).

Immune Response Driver in HBV-related liver cancer

To examine the relationship between TCR recognition and neoepitope sequence similarity to pathogen derived epitopes in samples that coexpress both, we examined patients with HBV infection and hepatocellular carcinoma from the LIHC TCGA dataset. We assessed 190 patients with matched WES and RNA-Seq data, detecting HBV transcripts in 115/190 (60%) via HBV genome assembly from RNAseq data unmapped to human genes (See Methods). Of these, 88 patients produced HBV matching protein sequences through ORFfinder. Using the RNA-seq data for patient HLA typing, we estimated the distribution of binding affinities of the viral antigens and compared it with that of neoantigens produced by tumor mutations. A total of 133,834 unique tumor neoepitopes and 30,357 HBV viral epitopes were predicted across the patients. Cumulative distribution functions of the predicted MHC-I binding affinity distributions indicate a significant MHC-I binding affinity preference for tumor derived neoantigens over that of HBV viral cofactors (**Fig. 1b, 4**). This result is robust against subsampling among neopeptides (see Methods and **Supp. Fig. 1**). In addition, we found that tumor neoepitope burden is lowly but significantly associated with patient TIL burden (Spearman's $\rho=0.24$,

$p=0.038$), but HBV epitope burden was not (restricting to MHC-I strong binders [$ic50 < 200$ nM]; **Supp. Fig. 2**), further suggesting that TIL recruitment is preferentially driven by relative neoepitope burden compared to viral burden.

Discussion

Determining the degree of ‘non-selfness’ of mutant peptides in the face of enormous individual variability of TCR repertoires is notoriously difficult, and yet critical, to answer at scale. Point somatic mutations located outside the MHC-binding anchor positions may appear to be more ‘non-self’ since they may lead to significantly increased peptide-MHC binding compared with wildtype sequence. However it has traditionally not been straightforward to translate this notion into a better survival or treatment response predictor. The relative spectra of subclonal and clonal immunogenic mutations, and similarly mutant sequence homology with experimentally validated pathogen epitopes, potentially contain important tumor evolution signatures, which may indicate intriguing similarities with pathogen evolution.

To gain further intuition into a recent neoepitope based tumor fitness scoring model (3), we applied it to samples from treatment-naive samples of the same tumor types in the TCGA. A key aim was to test how this model predicts survival given that it has shown promise in predicting response to immune checkpoint inhibitors. Although this setting may involve substantially different (thus far uncharacterized) tumor-immune dynamics, we reasoned that a sufficiently general notion of tumor fitness should correlate with patient survival, especially in those cohorts where TIL and CYT are already known as strong survival correlates.

Our results suggest that the proposed tumor fitness measure based on pathogen epitope similarity does not correlate with CYT in either NSCLC nor SKCM, potentially indicating that it is specific to the patients treated with checkpoint inhibitors. Furthermore, in the case of HBV-related HCC in the TCCA cohort, we find that even when viral epitopes are competing with neoantigens for presentation to T cells there is actually a substantial average bias towards higher MHC-I binding affinity for the neoepitopes. In addition, significant correlation between TMB and TIL burden further suggests that the tumor dominates immune recruitment over HBV viral epitopes. It is interesting to speculate on whether other tumors with known viral cofactors, such as cervical or head and neck with Human Papillomavirus, Epstein Barr virus and Burkitt’s lymphoma, show similar biases.

Furthermore, we find that tumor fitness in the treatment-naive samples does not improve prediction error of survival beyond that of TMB and clinical tumor staging alone, while a simple measure of CYT does so in SKCM. The tumor fitness model has two key degrees of freedom that could very likely be tuned to reduce this prediction error, as they were for patients treated with checkpoint inhibitors, but it is instructive to simply note here that these choices do not work well in untreated samples. These data suggest that the tumor immune dynamics in treated patients are notably

different than in untreated patients. It may also reflect a very cancer or dataset specific sensitivity of the tumor fitness score since the CYT measure alone seems to reduce survival prediction error, as found by others (23,24). Indeed, CYT alone is found to be a useful survival predictor in untreated patients and also a useful component to add to the tumor fitness score (as already noted by the authors).

Although our study points out key limitations in extending the paradigm of tumor fitness scoring to untreated patients, it does have some caveats. First, the accuracy of in-silico predictions of neoantigen or viral binding affinity in estimating immune reactivity are at best suboptimal compared to using mass spectroscopy. Similarly, in comparing viral and neo-epitopes it's important to note that several lines of evidence suggest that the replication status of HBV is dependent on the differentiation status of the cells (15,16). Thus, the virus may hardly replicate in HCC cells and further reduce the viral epitope burden within the tumor.

Overall our study indicates that while tumor fitness scores can be used to predict response to checkpoint inhibitors, they do not seem to predict survival in untreated patients where endogenous immune activation is a significant survival factor. Nevertheless, it is encouraging to observe that CYT measures are powerful in both treated and untreated patients, which may point to the existence of universally predictive and prognostic immune activation signatures.

Methods

TCGA analysis

RNA-Seq data for the TCGA patient cohorts was aligned to Hg38 with STAR (v2.5.1b) in two-pass mode (7). Gene counts for Gencode v23 (www.gencodegenes.org) gene annotations were generated using featureCounts. Read counts underwent TMM normalization and logCPM transformation using voom (17). Mapped reads were used to allelotype (MHC class-I loci) each patient (8), estimate the putative TIL burden per patient by profiling TCR and BCR sequences with MiXCR (9), and normalizing by patient library size. To predict neoantigen and associated epitope burden, we used Topiary (19) to call mutation-derived cancer T-cell epitopes from somatic variants, tumor RNA expression data, and patient class I HLA type. This tool matches mutations with gene annotations, filters out non-protein coding changes, and finally creates a window around amino acid changes, which is then fed into NetMHCCons for each patient HLA allele across tiles of 9-12 aa in length. Given that HLA-I processes neoantigens by degradation to non-conformational 8-11 amino-acid residues, we excluded neopeptides with mutations obscured to T-cells within HLA-I binding pockets. In the case of frameshift mutations, in principle this window starts from the mutation minus the length of the peptide up to the first stop codon. Predictions were filtered by a binding affinity threshold of $ic50 < 10000nM$. A measure of tumor

mutation burden (TMB) for each patient was calculated by enumerating the number of called DNA-mutations in patient associated MAF files.

Tumor fitness score

We assigned tumor immunogenicity scores following the method outlined by the model described in (3). Briefly, a protein BLAST of the neoepitopes from the SKCM and NSCLC cohorts was performed per patient against a database of viral epitopes sourced from the International Epitopes Database (IEDB)(21); the best hits with higher sequence similarity normalized by sequence database size (bitscore) for each neoepitope were retained. A second, randomized set of neoepitopes was also blasted, as a negative control group. Smith-Waterman alignments scores were calculated for each match. For each patient neoantigen, we calculated the TCR recognition potential score (R) and MHC-I binding affinity amplitude score (A), as a ratio of the binding affinities of the mutant neoepitope and the wild type epitope. Tumor immunogenicity was assigned by selecting the maximum of these scores from among all neoantigens, j :

$$\tilde{I} = \max(R_j, A_j) \quad (1)$$

This term represents the effective expected size of immune response and is used to rank the dominant immunogenic clone per patient. The inverse of this score serves as the tumor fitness score.

Cytolytic T-Cell activity (CYT) scores were calculated using the geometric mean of the FPKM (fragments per kilobase mapped) expression of granzyme (*GZMA*) and perforin-1 (*PRF1*) (10). Spearman correlations between patient tumor immunogenicity scores and CYT were calculated in R.

HBV antigen calling

Raw RNA sequencing reads that did not map to the GRCh38 reference genome was assembled into contigs using Trinity (using `-no_run_chrysalis -no_run_butterfly flags`, which only invokes the Inchworm step) to perform greedy kmer-25 contig assembly (11). Resulting contigs with a sufficiently high entropy (to exclude homopolymer sequences), at least 100 bp long and supported by at least 20 reads were retained and aligned with BLAST against the HBVdb (18) reference genomes (e-value < 1e-6) for HBV (genotypes A, B, C, D, E, G, and H), effectively identifying the HBV positive patients (n=115). CD-Hit was used to consolidate highly similar contig sequences (e-values < 1e-10) (12,13). Finally, ORFfinder was used to predict the putative HBV protein products from each contig, which were validated and filtered (e-value < 1e-10) by a protein BLAST against an HBV protein database compiled from HBVdb for the HBV genotypes above (14). Importantly, our contig length filtering means that ORFs shorter than 300 aa are excised. HBV epitopes were predicted using the matching protein products and patient HLA-typing calls with Topiary (see above),

and peptides were filtered by binding affinity ($ic_{50} < 10000nM$). Comparison of viral and neo-epitope MHC-I binding affinity distributions was performed using a one-sided Kolmogorov-Smirnov test.

Additionally, to assure that the MHC-I binding affinity bias toward tumor neoepitopes was not confounded by a larger epitope set, we subsampled 10000 epitopes from both populations and compared binding affinity distributions by one-sided (neoepitope greater) Kolmogorov-Smirnov test for 1000 iterations (**Supp. Fig. 1**).

Survival Analysis

Univariate (Kaplan-Meier) curves and risk tables using patient tumor immunogenicity, *I*, and immune activity, *CYT*, were created with the `ggsurvplot` package. Patient grouping into low and high tumor immunogenicity and immune activity was done using the bottom 15% and top (85%) 15% quantiles for these measures, respectively. A log-rank test was used to evaluate significance in predicted survival outcomes between groups. The relative predictive power of various survival models was evaluated using the `pec` R package (20) by computing the Integrated Brier Score (IBS) across bootstrap cross validation with 100 iterations ($B=100$). We used the Kaplan-Meier estimator for the censoring times in the cross validation simulations. The weights in the IBS correspond to the probability of not being censored. Model error curves were compared using Wilcoxon test for IBS comprising approximately 80% of total patients, with test significance provided in graphic tables (Figure 3c,d). IBS cross validation was performed by sampling Brier scores with 100 iterations across random patient groups for each model and applying a one-sided (TMB_I less) Kolmogorov-Smirnov test.

Availability of Code and Data: All code and non-protected data is available upon reasonable request to the corresponding author.

References

1. Sharma, P., Hu-Lieskovan, S., Wargo, J. A. & Ribas, A. Primary, Adaptive, and Acquired Resistance to Cancer Immunotherapy. *Cell* 168, 707–723 (2017).
2. Riaz, N. et al. Tumor and Microenvironment Evolution during Immunotherapy with Nivolumab. *Cell* 171, 934-949.e16 (2017).
3. Łuksza, M. et al. A neoantigen fitness model predicts tumour response to checkpoint blockade immunotherapy. *Nature* 551, 517–520 (2017).
4. Vita, R. et al. The Immune Epitope Database (IEDB): 2018 update. *Nucleic Acids Research* 47, D339–D343 (2019).
5. Havel, J. J., Chowell, D. & Chan, T. A. The evolving landscape of biomarkers for checkpoint inhibitor immunotherapy. *Nat. Rev. Cancer* 19, 133–150 (2019).
6. Rizvi, N. A. et al. Cancer immunology. Mutational landscape determines sensitivity to PD-1 blockade in non-small cell lung cancer. *Science* 348, 124–128 (2015).
7. Dobin, A. et al. STAR: ultrafast universal RNA-seq aligner. *Bioinformatics* 29, 15–21 (2013).

8. Szolek, A. HLA Typing from Short-Read Sequencing Data with OptiType. *Methods Mol. Biol.* 1802, 215–223 (2018).
9. Bolotin, D. A. et al. MiXCR: software for comprehensive adaptive immunity profiling. *Nat. Methods* 12, 380–381 (2015).
10. Rooney, M. S., Shukla, S. A., Wu, C. J., Getz, G. & Hacohen, N. Molecular and genetic properties of tumors associated with local immune cytolytic activity. *Cell* 160, 48–61 (2015).
11. Haas, B. J. et al. De novo transcript sequence reconstruction from RNA-seq using the Trinity platform for reference generation and analysis. *Nat. Protoc.* 8, 1494–1512 (2013).
12. Fu, L., Niu, B., Zhu, Z., Wu, S. & Li, W. CD-HIT: accelerated for clustering the next-generation sequencing data. *Bioinformatics* 28, 3150–3152 (2012).
13. Li, W. & Godzik, A. Cd-hit: a fast program for clustering and comparing large sets of protein or nucleotide sequences. *Bioinformatics* 22, 1658–1659 (2006).
14. Rombel, I. T., Sykes, K. F., Rayner, S. & Johnston, S. A. ORF-FINDER: a vector for high-throughput gene identification. *Gene* 282, 33–41 (2002).
15. Halgand, B., Desterke, C., Riviere, L., Fallot, G., Sebah, M., Calderaro, J., et al. Hepatitis B Virus Pregenomic RNA in Hepatocellular Carcinoma: A Nosological and Prognostic Determinant. *Hepatology*, 1, 86-96 (2018).
16. Fu, S., Li, N., Zhou, P. C., Huang, Y., Zhou, R. R., Fan, X. G. Detection of HBV DNA and antigens in HBsAg-positive patients with primary hepatocellular carcinoma. *Clin. Res. Hepatol. Gastroenterol.* 4, 415-423 (2017).
17. Ritchie, M. E., Phipson, B., Wu, D., Hu, Y., Law, C. W., Shi, W., Smyth, G. K. limma powers differential expression analyses for RNA-sequencing and microarray studies. *Nucleic Acids Research*, 7, e47 (2015).
18. Hayer, J., Jadeau, F., Deleage, G., Kay, A., Zoulim, F., Combet, C. HBVdb: a knowledge database for Hepatitis B Virus. *Nucleic Acids Research*, D1, D566-D570 (2013).
19. Rubinsteyn, A., Nathanson, T. Topiary: predict mutated T-cell epitopes from sequencing data. Github repository, <https://github.com/openvax/topiary> (2018)
20. Mogensen, U. B., Ishwaran, H., Gerds, T. A. Evaluating Random Forests for Survival Analysis using Prediction Error Curves. *J. Stat. Softw.* 50,1-23 (2012) URL: <http://www.jstatsoft.org/v50/i11/>
21. Vita, R., Mahajan, S., Overton, J. A., Dhanda, S. K., Martini, S., et al. The Immune Epitope Database (IEDB): 2018 Update. *Nucleic Acids Res.* (2018).
22. Barnes, T. A., Amir, E. HYPE or HOPE: the prognostic value of infiltrating immune cells in cancer. *Br J Cancer.* 4,451-460 (2017)
23. Wakiyama, H., Masuda, T., Motomura, Y., Hu, Q., Tobo, T., Eguchi, H., Sakamoto, K., et al. Cytolytic Activity (CYT) Score is a Prognostic Biomarker Reflecting Host Immune Status in Hepatocellular Carcinoma (HCC). *Anticancer Res.* 12, 6631-6638 (2018).
24. Roufas, C., Chasiotis, D., Makris, A., Efstathiades, C., Dimopoulos, C., Zaravinos, A. The Expression and Prognostic Impact of Immune Cytolytic Activity-Related Markers in Human Malignancies: A comprehensive Meta-analysis. *Front. Oncol.* 8, 27 (2018).

Figures:

Figure 1: A) Workflow summary. Matched mutation and RNA-seq TCGA datasets underwent HLA-Typing, neoepitope calling, and VDJ-alignment for each cohort, and tumor fitness scores calculated for those in the SKCM and NSCLC (3). Unmapped reads from the LIHC cohort were mined for HBV reads, which were used to predict viral epitopes. **B)** T-cell recognition by TCR of a cancer cell by MHC-I presentation. Antigens bound to the MHC can displace other antigens due to higher binding affinity with the MHC molecule. This competitive binding affinity is represented by an ic50 score.

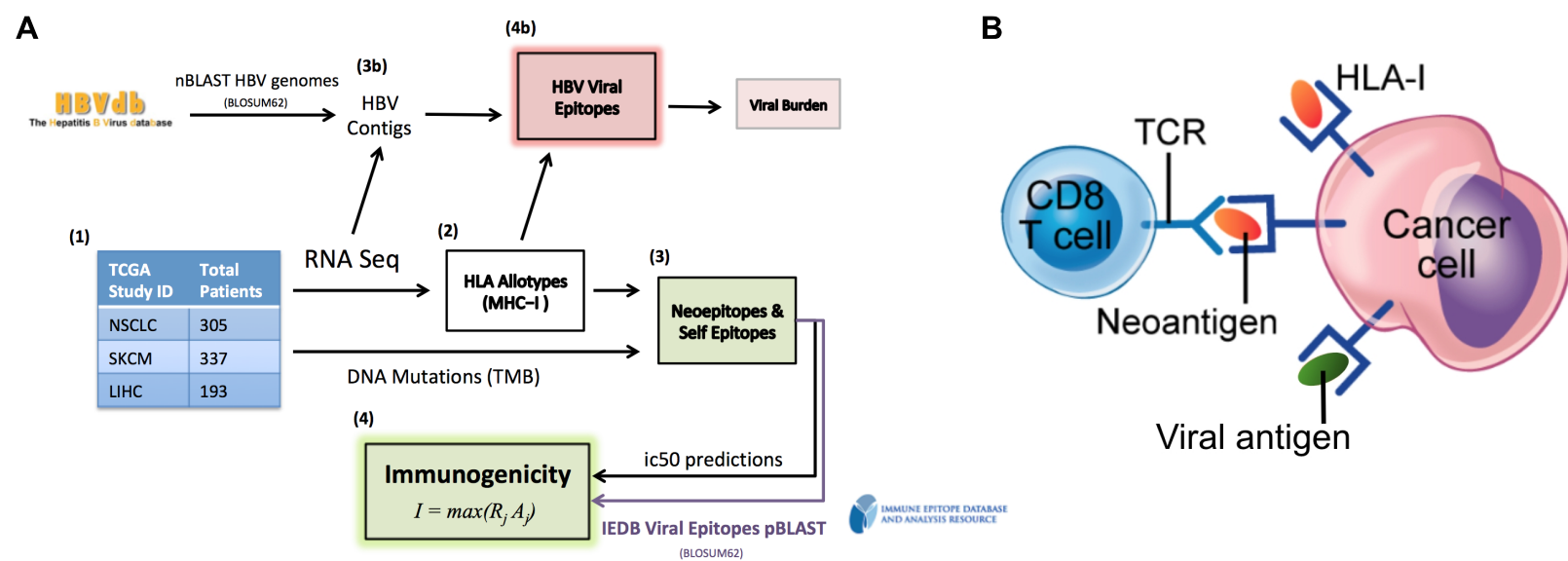


Figure 2: Maximal clonal immunogenicity (inverse tumor fitness), \bar{I} , was found to be lowly and non-significantly correlated (Spearman) with all our measures of expression-based tumor immune response (TIL burden, TIL clonality and CYT) and TMB in both **A) NSCLC**, **B) SKCM** patients. Several of the immune measures were found to be highly correlated with each other in both TCGA patient sets. Values in each circle indicate the spearman correlations between the features, with color and size representative of correlation strength. Tiles with no color indicate a non-significant ($p > 0.05$) correlation between features.

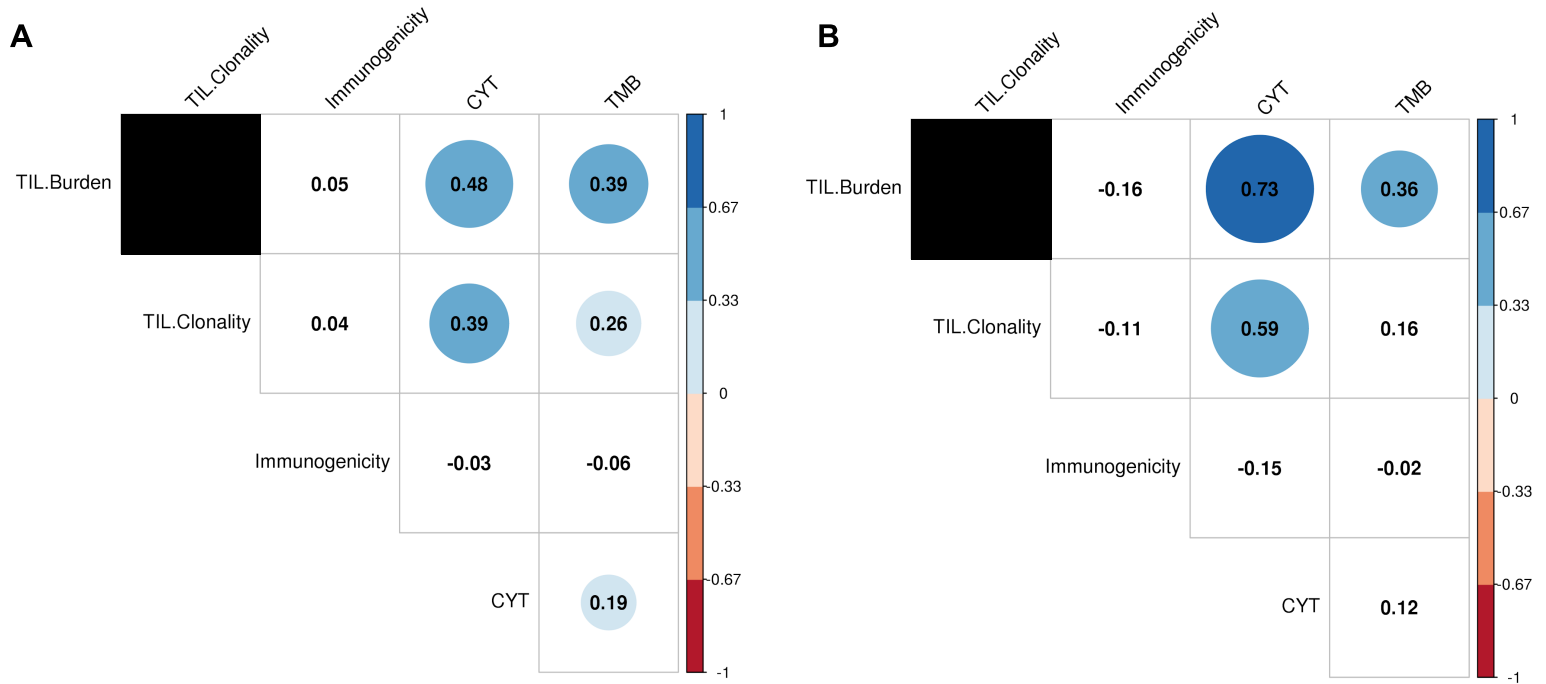


Figure 3: Univariate KM survival curves between patients grouped by highest and lowest immunogenicity (*I*) and immune activity marker expression (*CYT*) scores for the **A,B** lung (NSCLC) and **C,D** melanoma (SKCM) TCGA cohorts. Quantiles of *I* and *CYT* patient scores used to group cohorts with the lowest and highest groups represented by the curves; **E,F** Time dependent Brier scores (prediction error curves) comparing multivariate cox proportional hazard survival models for the NSCLC cohort (e), and SKCM cohort (f). Reference is intercept, all other models include tumor stage covariates. TMB includes patient tumor mutation burden, TMB_I includes immunogenicity and TMB, CYT_TMB includes CYT and TMB. Vertical lines demarcate approximately 80% of the patients, for which integrated Brier scores were calculated.

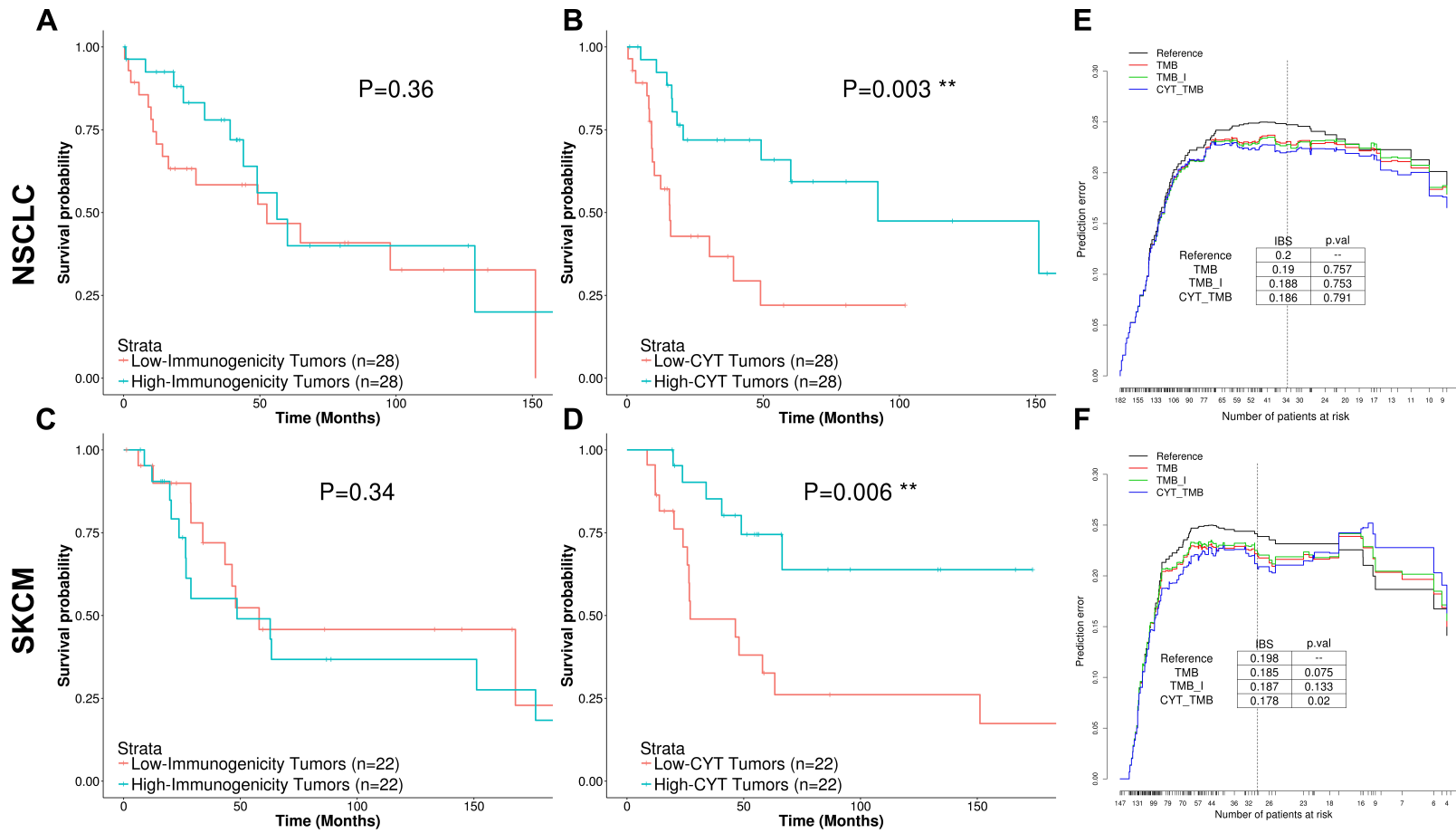


Figure 4 : Distribution of MHC-I binding affinities for tumor neoantigens (blue) and HBV antigens (red). Smaller ic50 values indicate a stronger binding affinity. Tumor neoantigens are on average more likely to bind to patient MHC-I alleles than antigens from HBV proteins.

